**New constraints on Northern Hemisphere growing season net flux**

Running title: Larger North Hemisphere Net Ecosystem Exchange

Z. Yang[1], R.A. Washenfelder[2,*], G. Keppel-Aleks[2], P.O. Wennberg[1,2], N.Y. Krakauer[1,#], J.T. Randerson[3], P.P. Tans[4] and C. Sweeney[5]

[1]Division of Geological and Planetary Science, California Institute of Technology, Pasadena, CA 91125; yangzh@gps.caltech.edu; 626-395-6293

[2]Division of Engineering and Applied Science, California Institute of Technology, Pasadena, CA 91125; wennberg@gps.caltech.edu

[3]Department of Earth System Science, University of California, Irvine, CA 92697; jranders@uci.edu

[4]Earth System Research Laboratory, National Oceanic and Atmospheric Administration, Boulder, CO 80305; Pieter.Tans@noaa.gov

[5]Cooperative Institute for Research in Environmental Sciences, University of Colorado, Boulder, CO 80309; Colm.Sweeney@noaa.gov

[*]Now at Chemical Sciences Division, Earth System Research Laboratory, NOAA, Boulder, CO 80305; Rebecca.Washenfelder@noaa.gov

[#]Now at Department of Earth and Planetary Science, University of California, Berkeley, CA 94720; niryk@berkeley.edu

Submitted to GRL: Feb 16, 2007

**Abstract**

Observations of the column-averaged dry molar mixing ratio of $CO_2$ above both Park Falls, Wisconsin and Kitt Peak, Arizona, together with partial columns derived from six aircraft profiles over Eurasia and North America are used to estimate the seasonal integral of net ecosystem exchange (NEE) between the atmosphere and the terrestrial biosphere in the Northern Hemisphere. We find that NEE is approximately 28% larger than predicted by the Carnegie Ames Stanford Approach (CASA) model. We show that the earlier estimates of NEE may have been biased low by too weak vertical mixing in the transport models used to infer seasonal changes in Northern Hemisphere $CO_2$ mass from the measured surface $CO_2$.

**Index Terms**: 0315 Atmospheric composition and structure: Biosphere/atmosphere interactions (0426, 1610); 0428 Biogeosciences: Carbon Cycling (4806);

Keywords: Northern Hemisphere, terrestrial carbon sink, net ecosystem exchange, column-averaged $CO_2$, aircraft profiles, inverse modeling

## 1. Introduction

Forecasting future $CO_2$ levels in the atmosphere is needed to predict future climate. Accurate forecasts require an improved understanding of carbon sources and sinks [*IPCC*, 2001]. During the 1990s, fossil fuel combustion and cement production added approximately 6 Pg C $yr^{-1}$ to the atmosphere. These fluxes are well constrained spatially and temporally [*Andres et al.*, 1996]. From the observed atmospheric increase and the known anthropogenic emissions, the combined ocean and terrestrial biosphere carbon sinks must have been close to 3 Pg C $yr^{-1}$ [*IPCC*, 2001].

To estimate the spatial and temporal distribution of these carbon sinks, inverse methods have been used to estimate carbon fluxes from geographically sparse observations of atmospheric $CO_2$ mixing ratio, typically measured at the surface (e.g. *Tans et al.* [1990]). In these methods, surface fluxes are scaled within the framework of a global atmospheric transport model to minimize the difference between the observed and simulated spatial and temporal gradients of atmospheric $CO_2$ mixing ratio [*Enting et al.*, 1995; *Kaminski et al.*, 1999; *Rayner et al.*, 1999; *Bousquet et al.*, 2000; *Krakauer et al.*, 2004; *Baker et al.*, 2006]. Estimates of both NEE and the geographical distribution of fossil fuel carbon sinks vary significantly, due in large part to errors in the atmospheric transport models used in these inversions (e.g. *Gurney et al.*, [2004]). This is quite understandable; estimation of fluxes on large geographical scales requires knowledge of temporal and spatial gradients in $CO_2$ mass. These changes in mass can be inferred from gradients in the observed mixing ratio at the surface only if the vertical structure of atmospheric $CO_2$ is well known. Proper simulation of the exchange between the planetary

boundary layer (PBL) and the free troposphere, however, is still an area of active research for the atmospheric dynamics community.

In this study, we use newly available observations of the column and vertical profile dry air $CO_2$ molar mixing ratios above eight sites (Table 1) to estimate the seasonally-varying carbon flux (NEE) in the northern hemisphere. Because these observations are of the column abundance, they come close to representing directly a measure of atmospheric $CO_2$ mass. As a result, our estimate of NEE is significantly less sensitive to errors in the vertical transport than estimates based solely on surface observations. Our analysis suggests that the seasonally-varying fluxes are substantially larger than the NEE fluxes from the CASA model used in the TransCom 3 studies. We show using vertically resolved observations of $CO_2$ obtained at several sites in Eurasia and North America that the TransCom models underestimate the seasonally-varying fluxes because they underestimate the efficiency of mixing of $CO_2$ throughout the free troposphere.

**2. Measurements and Models**

Measurements of column-averaged dry $CO_2$ were obtained at Park Falls, Wisconsin beginning in 2004. Using an automated solar observatory, direct solar spectra were acquired continuously during clear-sky, daytime conditions. These spectra were used to determine vertically integrated $CO_2$ mass with high precision (0.1%) [*Washenfelder et al.*, 2006]. The 337 days of measurements were taken during May 2004 to November 2006 and have been averaged daily. We also included similar but much infrequent (only 96 days during the two periods: Jan 1979 to Dec 1985 and Mar 1989 to Mar 1995) column measurements obtained at the Kitt Peak solar observatory, Arizona [*Yang et al.*,

2002]. In addition to the ground-based total columns, multi-level aircraft $CO_2$ measurements were available at six sites in North America and Eurasia during 2003-2004 (Table 1). Discrete $CO_2$ samples were acquired biweekly or monthly during aircraft profiles up to 7500 m above the surface (e.g. *Levin et al.* [2002]). In our analysis, we used the interpolations of these measurements at fixed temporal (48 per year) and spatial (every 500m in altitude) intervals [*GLOBALVIEW-$CO_2$*, 2006].

To compare with the observations, we used the twelve TransCom 3 experiment models that differ in spatial resolution, advection scheme, driving winds, and sub-grid scale parameterizations [*Gurney et al.*, 2003]. Monthly terrestrial biosphere exchange (1°×1°) was derived from the Carnegie-Ames-Stanford Approach (CASA) terrestrial biosphere model [*Randerson et al.*, 1997], and is annually balanced at each grid cell.

## 3. Methods

In our analysis, we compared the observed amplitude and phase of the atmospheric $CO_2$ seasonal cycles to simulations obtained from propagating seasonal surface fluxes from a terrestrial biosphere model (CASA) with annually-balanced fluxes through the twelve different transport models. Since the same fluxes are used, differences in the simulated atmospheric $CO_2$ seasonal cycles at different altitudes and locations become a comparative measure of differences in transport in the models. To quantify the differences between the observations and the simulations, we used a simple least square fit, assuming the observed seasonal cycle $S(t)$ was a function of the simulated CASA biosphere model response $S_0(t)$, adjusted by scale $A$, time delay $T$, and offset $B$:

$$S(t) = A \times S_0(t-T) + B$$

Focusing on the shape of seasonal cycle, we reported $A$ and $T$ but not offset $B$. Besides the simulations from the twelve models, the mean of all these models' simulations was considered as our "best" estimate and included in the comparison. The fitting rms ($\sigma$) for the all-model mean simulation was reported to measure the goodness of the fit, and to derive a weighted mean CASA scale factor (but not time delay) for $n$ different sites:

$$\overline{A} = \frac{\sum_{i=1}^{n} A_i / \sigma_i^2}{\sum_{i=1}^{n} 1 / \sigma_i^2}$$

To compare the observations with the neutral biosphere simulations, the measurements had been detrended and offset by the annual mean value. The interannual trend for the Park Falls column $CO_2$ was empirically determined as 1.80 ppm $yr^{-1}$ during 2004 to 2006. For Kitt Peak, the trends were 1.41 ppm $yr^{-1}$ during 1979 to 1985 and 0.83 ppm $yr^{-1}$ during 1989 to 1995. For the temporally evenly spaced GlobalView assimilations, their seasonal cycles were directly decomposed using the empirical mode decomposition method [*Huang et al.*, 1998] and folded into one year.

**4. Results and Discussion**

The comparison between the Park Falls $CO_2$ seasonal cycle of column-averaged observation and the TransCom simulations is shown in Figure 1. The observed seasonal $CO_2$ cycle amplitude is larger than any model simulation. A best fit was obtained by increasing the CASA fluxes by 34%. Models also underestimated the $CO_2$ seasonal cycle at Kitt Peak and all the other six aircraft sites (average difference of 27%, Table 1). Because these vertically-integrated observations sample a significant fraction of the northern

hemisphere landmass, they provide a measure of $CO_2$ mass variations that is not highly sensitive to error in the transport fields. As a group, the seasonal cycle in column $CO_2$ is most sensitive to the seasonal fluxes themselves. This is supported by the relatively small variation in the model simulations of the columns illustrated for Park Falls in Figure 1 and for the other sites in the accompanying supplementary material[1].

The NEE used in CASA was derived from 1990 satellite observations, and so the observed 0.66% $yr^{-1}$ increase rate of $CO_2$ seasonal-signal amplitude between 1981 to 1995 [*Randerson et al.*, 1997] may explain some, but clearly not all, of the differences between the observations and simulations of the amplitude of the $CO_2$ seasonal cycle. In addition, the phase analysis of $CO_2$ seasonal cycles shown in Table 1 shows that for all sites except Kitt Peak, CASA fluxes needed to be shifted earlier by one to three weeks, which may, in part, be explained by advances in the timing of spring thaw since 1988 [*Smith et al.*, 2004].

In contrast to the column results, comparison of the simulations of the seasonal cycle with $CO_2$ observations obtained at the surface (GLOBALVIEW-$CO_2$ flasks) between 30°N to 70°N shows a smaller under-estimation of seasonal cycle (~12%, Table 1) and a smaller phase delay ($T_{surface}$ = -11.9 days; $T_{column}$ = -14.5 days). Both the amplitude and phase differences between the estimates from surface and column observations suggest that the TransCom models as a group do not mix the surface fluxes into the free troposphere quickly enough.

To investigate vertical mixing in the models, we focused on altitude-resolved data from the six aircraft sites. Directly comparing the simulations and observations for these sites using the same analysis method as described above was hampered by large mis-

matches in the shape of the $CO_2$ seasonal cycle at some sites (e.g. ZOT in figure 2). [The results of such an analysis are shown in the online supplement[1]; the retrieved CASA scale factors increase with altitude, but the increase is not statistically significant].

To minimize the impact of the seasonal-signal shape mismatch we performed self-similarity tests separately for observations and model simulations, among their seasonal cycles at different altitudes. For each site, we defined a reference level and assumed the seasonal cycles $S(t)$ at any level could be represented by this reference seasonal cycle $S_{ref}(t)$ with a time delay $T$ (due to vertical mixing), amplitude scale factor $A$, and offset $B$, where $S(t)$ and $S_{ref}(t)$ must be of the same type (simulation or observation):

$$S(t) = A \times S_{ref}(t-T) + B$$

The 3500 m level was chosen as the reference for all sites. The comparison for each site is shown in Figure 2 and the retrieved values of $A$ and $T$ are listed in Table 2. For the model simulations at all sites, the scale factors monotonically decrease with altitude, while the time delays monotonically increase. In contrast, for the observations at or above 2500 m, all sites except ESP showed slower decreases or even increases in the amplitude scale factor with altitude as well as shorter delay, and even advance (at PFA) in the seasonal cycle phase. For levels below 2500 m, the observations showed mixed trends from site to site, again possibly influenced by strong PBL variation. The observation-model differences above 2500m strongly suggest that the atmospheric vertical and/or meridional mixing within the free troposphere is faster than the TransCom simulations.

## 5. Summary and implications

Comparison of the column-averaged $CO_2$ dry volume mixing ratio measurements and the TransCom models show that the CASA model underestimates the Northern Hemisphere growing season net fluxes by approximately 28%. Using multi-level observed $CO_2$ from the Northern hemisphere to diagnose the model performance at different altitudes, we identify substantial underestimation of free troposphere vertical mixing rates by TransCom models. While the mixing between the PBL and the free troposphere has been a major focus of carbon flux inversion experiments (i.e. TransCom), this analysis suggests that equally large errors exist in the rate of vertical mixing throughout the free troposphere.

The weak vertical exchange of the TransCom models will have impacts beyond the estimation of NEE. *Gurney et al.* [2004] have shown, for example, that the inferred uptake of fossil fuel carbon by land in the Northern Hemisphere by the various TransCom models (from 0.0 to 4.0 Pg C/yr depending on which transport model is used) is correlated with their estimate of the $CO_2$ seasonal cycle produced by the biosphere fluxes. Gurney et al. suggest that this correlation is consistent with errors in parameterization of the seasonal mixing efficiency between the planetary boundary layer (PBL) and the free troposphere (FT), which co-varies in time with the surface carbon exchange direction and strength [*Denning et al.*, 1995]. Our finding suggests that as a group, the TransCom models may have too little vertical mixing and so may overestimate the size of the Northern Hemisphere land sink. The validity of this inference, however, depends in part on the how the transport errors vary seasonally – something this study has not addressed.

The analysis described in this letter illustrates the utility of having information about the vertical distribution of $CO_2$ from aircraft. In addition, the total column meas-

urements allow a more continuous record of $CO_2$ mass. The Total Carbon Column Observing Network (TCCON) is being established to expand the number of sites where $CO_2$ columns are measured (data available at http://www.tccon.caltech.edu). TCCON will include a number of sites in both the Northern and Southern Hemispheres. These observations should provide an improved measure of the gradient in $CO_2$ mass between the Hemispheres. Based on the findings of this study, we expect that the N-S gradient will be larger than predicted by the TransCom inversions tied to surface observations.

## 6. Acknowledgements

We thank the TransCom 3 modeling community (K. Gurney, M. Prather, T. Maki, L. Bruhwiler, Y. Chen, R. Law, C. Yuen, S. Fan, M. Heimann, and D. Baker) for making the results of their simulations publicly available. This work was supported by a NASA grant NNG05GD07G. N. Y. Krakauer was supported by Graduate Fellowships from both NASA Earth and Space Science and the Betty and Gordon Moore foundation. Column $CO_2$ data from the Park Falls installation is available at www.tccon.caltech.edu.

**Reference**

Andres, R. J., et al. (1996), A 1 degrees × 1 degrees distribution of carbon dioxide emissions from fossil fuel consumption and cement manufacture, 1950-1990, *Global Biogeochem. Cycles*, *10*, 419-429.

Baker, D. F., et al. (2006), TransCom 3 inversion intercomparison: Impact of transport model errors on the interannual variability of regional $CO_2$ fluxes, 1988-2003, *Global Biogeochem. Cycles*, *20*, GB1002, doi:10.1029/2004GB002439.

Bousquet, P., et al. (2000), Regional changes in carbon dioxide fluxes of land and oceans since 1980, *Science*, *290*, 1342-1346.

Denning, A. S., et al. (1995), Latitudinal Gradient of Atmospheric $CO_2$ Due to Seasonal Exchange with Land Biota, *Nature*, *376*, 240-243.

Enting, I. G., et al. (1995), A Synthesis Inversion of the Concentration and $\delta^{13}C$ of Atmospheric $CO_2$, *Tellus, Ser. B*, *47*, 35-52.

GLOBALVIEW-$CO_2$ (2006), *Cooperative Atmosphere Data Integration Project - Carbon Dioxide*, CD-ROM, NOAA GMD (Boulder, Colorado; anonymous FTP to ftp.cmdl.noaa.gov, Path: ccg/co2/GLOBALVIEW).

Gurney, K. R., et al. (2002), Towards robust regional estimates of $CO_2$ sources and sinks using atmospheric transport models, *Nature*, *415*, 626-630.

Gurney, K. R., et al. (2003), TransCom 3 $CO_2$ inversion intercomparison: 1. Annual mean control results and sensitivity to transport and prior flux information, *Tellus, Ser. B*, *55*(2), 555-579.

Gurney, K. R., et al. (2004), Transcom 3 inversion intercomparison: Model mean results for the estimation of seasonal carbon sources and sinks, *Global Biogeochem. Cycles*, *18*, GB1010, doi: 10.1029/2003GB002111.

Huang, N. E., et al. (1998), The empirical mode decomposition and the Hilbert spectrum for nonlinear and non-stationary time series analysis, *Proc. Royal Society London, Ser. A*, *454*, 903-995.

IPCC (2001), *IPCC Third Accessment Report (TAR): Climate Change 2001*, Intergovernmental Panel on Climate Change.

Kaminski, T., et al. (1999), A coarse grid three-dimensional global inverse model of the atmospheric transport - 2. Inversion of the transport of $CO_2$ in the 1980s, *J. Geophys. Res.*, *104*, 18555-18581.

Krakauer, N. Y., et al. (2004), Using generalized cross-validation to select parameters in inversions for regional carbon fluxes, *Geophys. Res. Lett.*, *31*, L19108, doi: 10. 1029/ 2004GL020323.

Levin, I., et al. (2002), Three years of trace gas observations over the EuroSiberian domain derived from aircraft sampling - a concerted action, *Tellus, Ser. B*, *54*, 696-712.

Randerson, J. T., et al. (1997), The contribution of terrestrial sources and sinks to trends in the seasonal cycle of atmospheric carbon dioxide, *Global Biogeochem. Cycles*, *11*(4), 535-560.

Rayner, P. J., et al. (1999), Reconstructing the recent carbon cycle from atmospheric $CO_2$, $\delta^{13}C$ and $O_2/N_2$ observations, *Tellus, Ser. B*, *51*, 213-232.

Smith, N. V. et al. (2004), Trends in high northern latitude soil freeze and thaw cycles from 1988 to 2002, *J. Geophys. Res.*, *109*, D12101, doi: 10.1029/2003JD004472.

Tans, P. P., et al. (1990), Observational Constraints on the Global Atmospheric $CO_2$ Budget, *Science*, *247*, 1431-1438.

Washenfelder, R. A., et al. (2006), Carbon dioxide column abundances at the Wisconsin Tall Tower site, *J. Geophys. Res.*, *111*, D22305, doi: 10.1029/2006JD007154.

Yang, Z. H., et al. (2002), Atmospheric $CO_2$ retrieved from ground-based near IR solar spectra, *Geophys. Res. Lett., 29*(9), 1339, doi: 10.1029/2001GL014537.

Actual size (black and white)

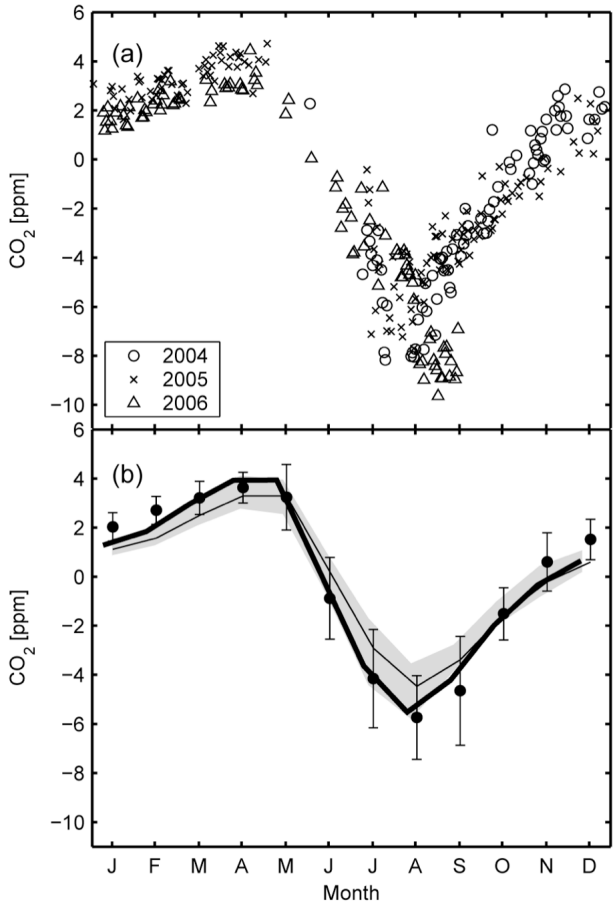


**Figure 1.** (a) Atmospheric column-average $CO_2$ mole fractions at Park Falls for May 2004 – March 2006. (b) The monthly mean of observations (close circles) compared with the TransCom simulations (grey shade show range of 12-model predictions; thin solid line represents average; thick solid line is the best fit). Each of the 12 models underpredicts the seasonal cycle observed in the column measurements. The best match to the observations is achieved by scale the model-mean simulations by 1.34 and shift them 7 days earlier.

Actual size (color)

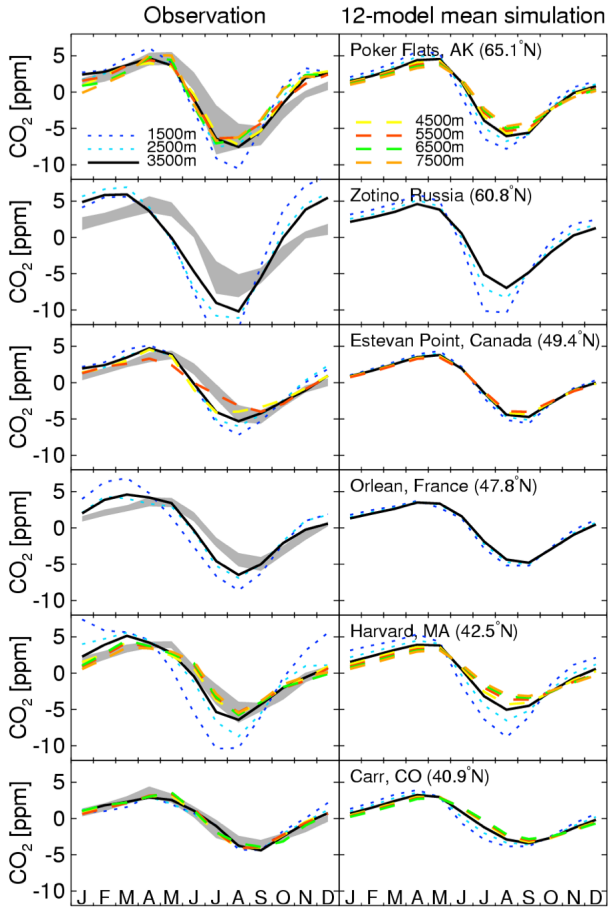


**Figure 2.** Comparison of the $CO_2$ seasonal cycles at different levels, for both the aircraft observations (left panel) and the TransCom 12-model mean simulation (right panel). Each altitude level is represented by a different line and each row represents one site respectively. The range of model simulations for 3500 meters altitude is also shown in the left panel as the shaded area.

**Table 1.** Column and profile observation sites and the $CO_2$ seasonal cycle amplitude comparison with model simulations

| Site Name (Code) | Location | Altitude range above surface (m) | Scale factor *A* of 12 models [a,b] | Phase Shift *T* of 12 models (days) | Scale factor *A* for the mean response of 12 models | RMS in fitting the mean response of 12 models (ppm) |
|---|---|---|---|---|---|---|
| Poker Flats, AK (PFA) | 65.07°N, 147.29°W | 1500-7500 | 1.20±0.11 | -16.8±4.5 | 1.21 | 0.71 |
| Zotino, Russia (ZOT) | 60.75°N, 89.38°E | 500-3500 | 1.44±0.21 | -18.4±2.8 | 1.42 | 1.70 |
| Estevan Point, Canada (ESP) | 49.38°N, 126.55°W | 500-5500 | 1.20±0.12 | -16.0±3.2 | 1.20 | 0.54 |
| Orleans, France (ORL) | 47.80°N, 2.50°E | 500-3500 | 1.39±0.18 | -19.6±3.1 | 1.38 | 0.43 |
| Park Falls, WI (LEF) | 45.93°N, 90.27°W | Total column | 1.34±0.14 | -7.3±4.0 | 1.34 | 0.43 |
| Harvard Forest, MA (HFM) | 42.54°N, 72.17°W | 500-7500 | 1.38±0.09 | -16.0±2.7 | 1.38 | 0.67 |
| Carr, CO (CAR) | 40.90°N, 104.80°W | 1500-6500 | 1.20±0.11 | -7.6±7.3 | 1.21 | 0.56 |
| Kitt Peak, AZ [c] (KTP) | 31.90°N, 111.60°W | Total column | 1.11±0.07 | 15.3±4.6 | 1.12 | 0.56 |
| Mean | | | 1.28 | -14.5±5.0 [d] | 1.28 | 0.70 |
| Mean of 35 surface sites [e] in 30°N~70°N | | | 1.12 | -11.9±9.8 | 1.11 | 1.07 |

[a] For LEF and KTP, total $CO_2$ columns were simulated to do the comparison. For the aircraft sites, only partial columns with measurements are simulated.
[b] The names of the models are CSU.gurney, GISS.prather, GISS.prather2, GISS.prather3, JMA-CDTM.maki, MATCH.bruhwiler, MATCH.chen, MATCH.law, RPN.yuen, SKYHI.fan, TM3.heimann, GCTM.baker. For more detail refer to TransCom website (http://www.purdue.edu/transcom/) and Gurney et al. 2003.
[c] The Kitt Peak observations were taken from Jan 1979 to Mar 1995, for more detail refer to Yang et al., 2002.
[d] Excluding Kitt Peak due to different observation time period
[e] These surface sites are part of the Globalview-$CO_2$ (2006) network, for a detailed list see online supplement[1]

**Table 2.** The optimal values of (a) scale factor and (b) time delay in days applied to 3500 meters level seasonal $CO_2$ change for best matching the other levels. For each site, the left column is for the observations and the right column is for the 12-model mean simulations.

| | PFA | | ZOT | | ESP | | ORL | | HFM | | CAR | |
|---|---|---|---|---|---|---|---|---|---|---|---|---|
| (a) | Optimal values for scale factor *A* | | | | | | | | | | | |
| Altitude | Obs | Mod. | Obs. | Mod. | Obs. | Mod. | Obs. | Mod. | Obs. | Mod. | Obs. | Mod. |
| 7500m | 0.88 | 0.80 | | | | | | | 0.78 | 0.74 | | |
| 6500m | 0.93 | 0.85 | | | | | | | 0.87 | 0.78 | 1.05 | 0.90 |
| 5500m | 0.89 | 0.90 | | | 0.74 | 0.91 | | | 0.83 | 0.84 | 1.00 | 0.94 |
| 4500m | 0.92 | 0.95 | | | 0.89 | 0.95 | | | 0.85 | 0.91 | 1.05 | 0.98 |
| 3500m | 1.00 | 1.00 | 1.00 | 1.00 | 1.00 | 1.00 | 1.00 | 1.00 | 1.00 | 1.00 | 1.00 | 1.00 |
| 2500m | 1.03 | 1.12 | 1.18 | 1.20 | 1.07 | 1.07 | 1.03 | 1.06 | 1.25 | 1.23 | 0.98 | 1.12 |
| 1500m | 1.33 | 1.30 | 1.32 | 1.51 | 1.24 | 1.16 | 1.41 | 1.12 | 1.67 | 1.57 | 0.96 | 1.26 |

| | PFA | | ZOT | | ESP | | ORL | | HFM | | CAR | |
|---|---|---|---|---|---|---|---|---|---|---|---|---|
| (b) | Optimal values for time delay *T* (days) | | | | | | | | | | | |
| Altitude | Obs. | Mod. | Obs. | Mod. | Obs. | Mod. | Obs. | Mod. | Obs. | Mod. | Obs. | Mod. |
| 7500m | -2.0 | 7.0 | | | | | | | 13.0 | 13.0 | | |
| 6500m | -4.0 | 6.0 | | | | | | | 11.0 | 10.0 | 3.0 | 12.0 |
| 5500m | -1.0 | 4.0 | | | 8.0 | 1.0 | | | 10.0 | 8.0 | -2.0 | 10.0 |
| 4500m | 0.0 | 2.0 | | | -3.0 | 1.0 | | | 6.0 | 4.0 | -4.0 | 8.0 |
| 3500m | 0.0 | 0.0 | 0.0 | 0.0 | 0.0 | 0.0 | 0.0 | 0.0 | 0.0 | 0.0 | 0.0 | 0.0 |
| 2500m | -5.0 | -4.0 | -4.0 | -5.0 | -4.0 | -1.0 | -5.0 | -3.0 | -6.0 | -6.0 | -4.0 | -8.0 |
| 1500m | -7.0 | -10.0 | -10.0 | -10.0 | -4.0 | -2.0 | -12.0 | -7.0 | -21.0 | -13.0 | -4.0 | -16.0 |

**Supplementary material**

Auxiliary Material Submission for Paper 2007GLXXXXXX

New constraints on Northern Hemisphere growing season net flux

Z. Yang (1), R.A. Washenfelder (2,*), G. Keppel-Aleks (2), P.O. Wennberg (1,2), N.Y. Krakauer (1,#), J.T. Randerson (3), P.P. Tans (4) and C. Sweeney (5)

(1) Division of Geological and Planetary Science, California Institute of Technology, Pasadena, CA 91125; yangzh@gps.caltech.edu; 626-395-6293

(2) Division of Engineering and Applied Science, California Institute of Technology, Pasadena, CA 91125; wennberg@gps.caltech.edu

(3) Department of Earth System Science, University of California, Irvine, CA 92697; jranders@uci.edu

(4) Earth System Research Laboratory, National Oceanic and Atmospheric Administration, Boulder, CO 80305; Pieter.Tans@noaa.gov

(5) Cooperative Institute for Research in Environmental Sciences, University of Colorado, Boulder, CO 80309; Colm.Sweeney@noaa.gov

(*) Now at Chemical Sciences Division, Earth System Research Laboratory, NOAA, Boulder, CO 80305; Rebecca.Washenfelder@noaa.gov

(#) Now at Department of Earth and Planetary Science, University of California, Berkeley, CA 94720; niryk@berkeley.edu

Geophys. Res. Lett., xxx (xx), doi:10.1029/2007GLXXXXXX, 2007

**Introduction**

The figure "2007GLXXXXXX-fs01.eps" are used to illustrate our fits to the eight column and partial-column sites in Table 1. The figure "2007GLXXXXXX-fs02.eps" shows the CASA scale factors versus altitude. The table "2007GLXXXXXX-ts01.txt" is a list of the 35 surface sites in 30N-70N, from which the mean surface scale factor and phase shift were obtained.

**2007GLXXXXXX-fs01.eps**

The monthly mean of observations (open diamonds) compared with the TransCom simulations for each of the eight sites. In each figure, grey shade show range of 12-model predictions, thin dotted line represents average, and thick solid line is the best fit with scaling and shifting.

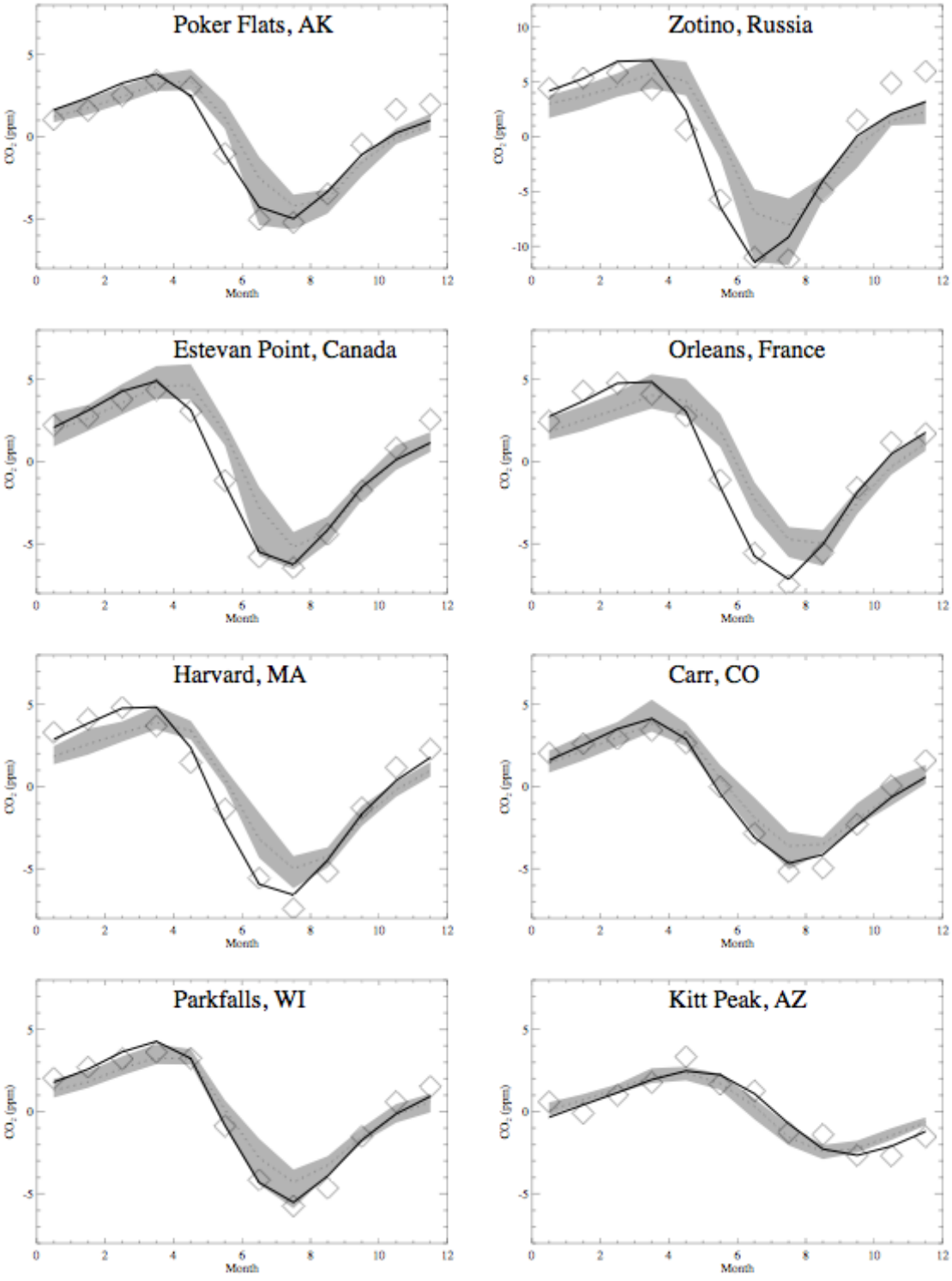
Poker Flats, AK
Zotino, Russia
Estevan Point, Canada
Orleans, France
Harvard, MA
Carr, CO
Parkfalls, WI
Kitt Peak, AZ
CO2 (ppm)
Month

**2007GLXXXXXX-fs02.eps**

The optimized scale factors A for CASA terrestrial biosphere model fluxes required for minimizing the difference between the observations and simulations at different altitudes. The A values of 12 model-mean are given at each of the six aircraft sampling sites (marked by different colors). The radius of each circle is proportional to 1/S^2, where S is the fit rms in ppm.

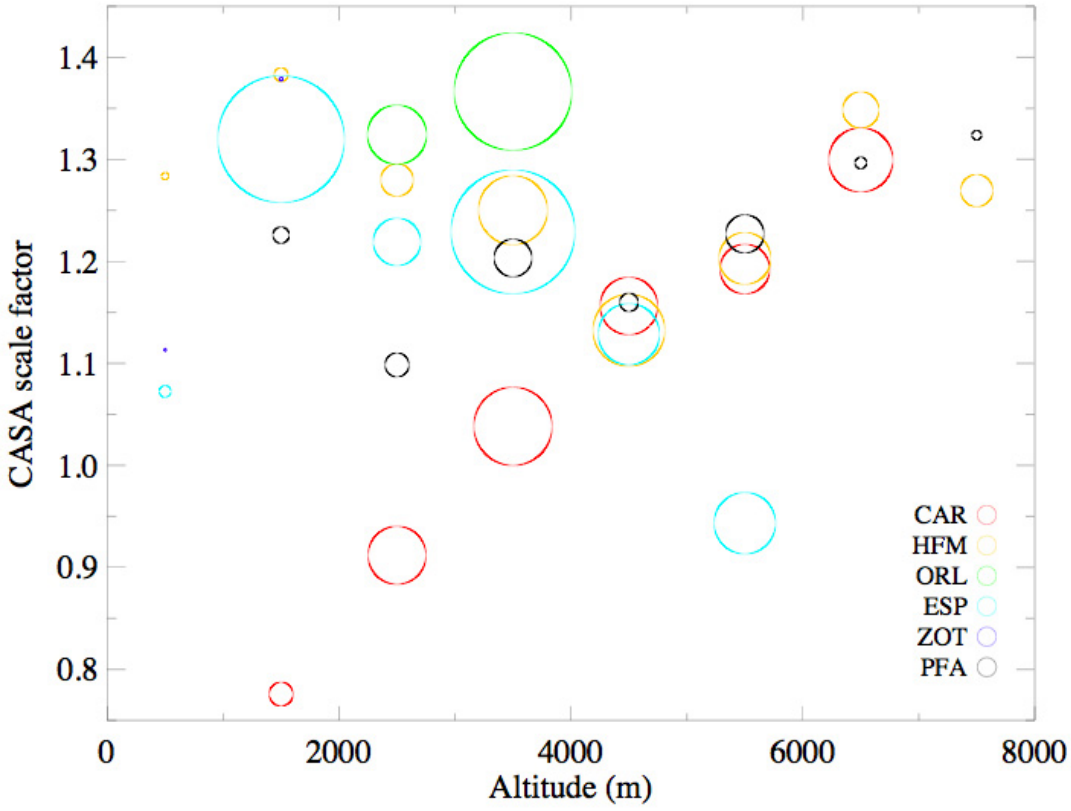

**2007GLXXXXXX-ts01.txt**

The list of 35 surfaces sites used for producing surface scale factor and phase shift in Table 1.

1.1 Column "Site", standard code name for GlobalView 2006 site.

1.2 Column "Type", land ("L") or ocean ("O") sites.

1.3 Column "Lat", degrees, site latitude.

1.4 Column "Lon", degrees, site longitude.

1.5 Column "Alt", meters, site altitude.

| Site | Type | Lat | Lon | Alt |
|---|---|---|---|---|
| bgu_11D0 | L | 41.83 | 3.33 | 30.00 |
| cmn_17C0 | L | 44.18 | 10.70 | 2165.00 |
| coi_20C0 | L | 43.15 | 145.50 | 100.00 |
| frd040_06C3 | L | 49.88 | -81.57 | 250.00 |
| hun_01D0 | L | 46.95 | 16.65 | 344.00 |
| kzd_01D0 | L | 44.45 | 77.57 | 412.00 |
| kzm_01D0 | L | 43.25 | 77.88 | 2519.00 |
| lef_01D0 | L | 45.93 | -90.27 | 868.00 |
| nwr_01D0 | L | 40.05 | -105.58 | 3475.00 |
| obs023_06C3 | L | 53.99 | -105.12 | 652.00 |
| palmbc_30C0 | L | 67.97 | 24.12 | 560.00 |
| pdm_11D0 | L | 42.93 | 0.13 | 2877.00 |
| prs_21C0 | L | 45.93 | 7.70 | 3480.00 |
| sch_23C0 | L | 48.00 | 8.00 | 1205.00 |

```
   uta_01D0  L    39.90  -113.72  1320.00
   uum_01D0  L    44.45   111.10   914.00
   wlg_01D0  L    36.29   100.90  3810.00
   azr_01D0  O    38.77   -27.38    40.00
   bal_01D1  O    55.50    16.67     7.00
   bme_01D0  O    32.37   -64.65    30.00
   bmw_01D0  O    32.27   -64.88    30.00
   bsc_01D0  O    44.17    28.68     3.00
   cba_01D0  O    55.20  -162.72    25.00
   esp_06D0  O    49.38  -126.55    39.00
   ice_01D0  O    63.25   -20.15   100.00
   lmp_28D0  O    35.52    12.62    45.00
   mhd_01D0  O    53.33    -9.90    25.00
pocn30_01D1  O    30.00  -126.00    10.00
   ryo_19C0  O    39.03   141.83   260.00
   sbl_06D0  O    43.93   -60.02     5.00
   shm_01D0  O    52.72   174.10    40.00
   sis_02D0  O    60.17    -1.17    30.00
   stm_01D0  O    66.00     2.00     7.00
   tap_01D0  O    36.73   126.13    20.00
   wis_01D0  O    31.13    34.88   400.00
```